

# PROCEEDINGS OF SPIE

[SPIDigitalLibrary.org/conference-proceedings-of-spie](https://SPIDigitalLibrary.org/conference-proceedings-of-spie)

## Deep convolutional neural network regularized digital breast tomosynthesis reconstruction with detector blur and correlated noise modeling

Gao, Mingjie, Fessler, Jeffrey, Chan, Heang-Ping

Mingjie Gao, Jeffrey A. Fessler, Heang-Ping Chan, "Deep convolutional neural network regularized digital breast tomosynthesis reconstruction with detector blur and correlated noise modeling," Proc. SPIE 12031, Medical Imaging 2022: Physics of Medical Imaging, 1203108 (4 April 2022); doi: 10.1117/12.2611933

**SPIE.**

Event: SPIE Medical Imaging, 2022, San Diego, California, United States

# Deep Convolutional Neural Network Regularized Digital Breast Tomosynthesis Reconstruction with Detector Blur and Correlated Noise Modeling

Mingjie Gao<sup>\*a,b</sup>, Jeffrey A. Fessler<sup>a,b</sup>, Heang-Ping Chan<sup>a</sup>

<sup>a</sup>Department of Radiology, University of Michigan, Ann Arbor, MI 48109; <sup>b</sup>Department of Electrical Engineering and Computer Science, University of Michigan, Ann Arbor, MI 48109

## Abstract

Digital breast tomosynthesis (DBT) reconstruction is an ill-posed inverse problem due to the limited-angle acquisition geometry. DBT is also a low dose imaging technique and has very noisy projection views. In this study, we investigated the feasibility of improving image quality of DBT reconstruction by combining (1) a model-based iterative reconstruction (MBIR) method that models the detector blur and correlated noise (DBCN) of the DBT system, and (2) a deep convolutional neural network based DBT denoiser, DNGAN, that we developed in our previous work. DBCN is physics-based whereas DNGAN is data-driven. We followed the regularization by denoising (RED) framework to construct a regularizer from DNGAN and used the DBCN-modeled terms in the MBIR formulation. We solved the optimization problem using the proximal gradient method. The proposed approach, named DBCN+DNGAN, was tested on a set of human subject DBT data sets. The image quality was evaluated quantitatively with figures of merit (FOMs) including the contrast-to-noise ratio, full width at half maximum, and task-based detectability index of a set of microcalcifications individually marked in the human subject data set. We found that these FOMs were improved in the DBCN+DNGAN-reconstructed DBT volumes compared to those reconstructed with DBCN alone or with the simultaneous algebraic reconstruction technique. The soft tissue appearance was visually satisfactory and the background noise level was low in the DBCN+DNGAN reconstructed images.

*Keywords:* deep learning, digital breast tomosynthesis, image reconstruction, microcalcification

## 1 INTRODUCTION

Digital breast tomosynthesis (DBT) is an x-ray imaging modality for breast cancer screening. A DBT scan acquires a small number of low dose mammograms while moving the x-ray source over a limited angular range. Reconstruction from the limited-angle acquisition produces tomographic image volumes with superior resolution in the slices parallel to the detector and reduces tissue overlaps in the depth direction [1]. From an image reconstruction point of view, however, the limited-angle design makes the DBT reconstruction an ill-posed inverse problem. Moreover, the total x-ray exposure of a DBT scan is set to be about the same as a single conventional digital mammogram, leading to very noisy projection view (PV) data. As a result, the reconstructed DBT is relatively noisy, which may obscure the detection of subtle signs of malignancy such as microcalcifications (MCs).

Model-based iterative reconstruction (MBIR) is an image reconstruction technique that considers the physics and photon statistics of the imaging system and has been demonstrated to improve image quality [2]. Zheng *et al.* developed an MBIR method for DBT that models the detector blur and correlated noise (DBCN) and achieved promising results using an edge-preserving regularizer [3]. In the past decade, the machine learning field has witnessed great success in data-driven deep learning methods such as deep convolutional neural networks (DCNN) for many applications including image denoising and reconstruction. We recently developed a DCNN-based denoiser called DNGAN for denoising DBT images [4][5].

In this work, we investigated the feasibility of combining DBCN and DNGAN, which we call DBCN+DNGAN, to take advantage of the benefits of both methods. We started from the DBCN formulation and constructed a regularizer from DNGAN for DBT reconstruction. We trained a suite of DNGAN denoisers with digital phantom DBT images and evaluated the proposed method using human subject DBTs.

---

\* Corresponding author: gmingjie@umich.edu

## 2 METHODS AND MATERIALS

### 2.1 DBCN+DNGAN Reconstruction

Conventional MBIR formulates image reconstruction as an optimization problem

$$\hat{x} = \underset{x}{\operatorname{argmin}} L(x) + \beta \cdot R(x) \quad (1)$$

where  $x$  is the unknown image,  $L(x)$  is the data fidelity term that usually includes the forward model of the imaging system and the measurement data,  $R(x)$  is the regularization term that reflects our prior knowledge on the image,  $\beta$  is the regularization parameter.

The DBCN method for DBT reconstruction incorporates the detector blur and correlated noise model into the data fidelity term and employs an edge-preserving regularizer to control the noise level [3]

$$L_{\text{DBCN}}(x) = \frac{1}{2} \sum_{i=1}^{N_p} \|y_i - BA_i x\|_{(BK_{q,i}B' + K_r)^{-1}}^2, \quad R_{\text{EP}}(x) = \sum_j \eta(\nabla x_j) \quad (2)$$

where  $N_p$  is the number of PVs,  $A_i$  is the system matrix of the  $i$ th scan angle,  $y_i$  is the  $i$ th PV,  $B$  is the detector blur matrix,  $K_{q,i}$  is the diagonal quantum noise matrix of the  $i$ th scan angle,  $K_r$  is the diagonal readout noise matrix,  $j$  indexes over all image voxels,  $\nabla$  is the finite difference operator that considers the 8 neighboring voxels within a DBT slice [6],  $\eta(t) = \delta^2(\sqrt{1 + (t/\delta)^2} - 1)$  is the hyperbola potential function.

In an effort to exploit the DNGAN denoiser in the DBCN reconstruction, we followed the regularization by denoising (RED) framework [7] and investigated the following additional data-driven regularizer for DBT

$$R_{\text{RED}}(x) = \frac{1}{2} \langle x, x - D(x) \rangle \quad (3)$$

where  $D(\cdot)$  denotes the pre-trained DNGAN denoiser,  $\langle \cdot, \cdot \rangle$  represents the inner product of the two images. Intuitively, this regularizer encourages either the denoising residual or the cross-correlation of the residual to the image to be small.

Now the overall optimization problem for the reconstruction becomes

$$\hat{x} = \underset{x}{\operatorname{argmin}} L_{\text{DBCN}}(x) + \beta_{\text{EP}} \cdot R_{\text{EP}}(x) + \beta_{\text{RED}} \cdot R_{\text{RED}}(x). \quad (4)$$

We solved the optimization problem using the proximal gradient method for RED (RED-PG) [8], using the gradient approximation described in [7]. The updates of the image variable  $x$  and the auxiliary variable  $z$  are given by

$$x_n = \underset{x}{\operatorname{argmin}} L(x) + \beta_{\text{EP}} \cdot R_{\text{EP}}(x) + \frac{\beta_{\text{RED}}}{2} \|x - z_{n-1}\|^2 \quad (5)$$

$$z_n = D(x_n) \quad (6)$$

where  $n$  is the iteration index. We solved the inner minimization problem (5) using the ordered subset version of the preconditioned gradient descent (OS-PGD).

### 2.2 DNGAN Training, Data Set and Figures of Merit

The noise level of DBT varies among patients. We trained a suite of DNGAN denoisers with digital phantom DBT images [9] generated for wide ranges of breast thicknesses, breast densities, and x-ray exposures. During reconstruction, the program estimated the DBT noise level and adaptively chose a matched denoiser for deployment.

We tested the DBCN+DNGAN reconstruction method on a data set consisting of 9 human subject DBT volumes. The DBTs were acquired with a prototype DBT system (GEN2, GE Global Research) that took 21 PVs within 60°. To simulate low dose scans and the current commercial DBT systems that use narrow-angle scanning, we used only the

central 9 PVs corresponding to  $24^\circ$  in our experiments. A total of 301 individual MCs were manually marked in the 9 DBT volumes. We calculated the contrast-to-noise ratio (CNR), full width at half maximum (FWHM), and task-based detectability index ( $d'$ ) on the focal plane of each marked MC [4] as figures of merit (FOMs) to quantify the conspicuity of the individual MCs and to compare different reconstruction algorithms.

### 3 RESULTS

Figure 1(a) shows the scatter plots of CNR, FWHM, and  $d'$  for DBCN+DNGAN versus simultaneous algebraic reconstruction technique (SART), which is an unregularized algorithm. The averaged CNR of the MCs for DBCN+DNGAN was improved by 115.5% ( $p < 0.0001$ , two-tailed paired t-test) compared to that for SART. The averaged FWHM was reduced (i.e., sharper) by 7.5% ( $p = 0.045$ ). The averaged  $d'$  was improved by 87.8% ( $p < 0.0001$ ).

DBCN was able to improve the image quality substantially compared to SART [3]. The proposed DBCN+DNGAN was able to advance it even further, as shown by the scatter plots for DBCN+DNGAN versus DBCN in Figure 1(b). The averaged CNR and averaged  $d'$  were improved by 24.3% and 28.5%, respectively ( $p < 0.0001$  for both FOMs). It is also worth noting that nearly all data points in the CNR or  $d'$  scatter plots, especially for those with lower values representing smaller MCs, were above the diagonal line. The FWHM decreased by an average of 14.1% ( $p < 0.0001$ ), indicating that the MCs were sharper in the DBCN+DNGAN reconstructed images than in the DBCN images.

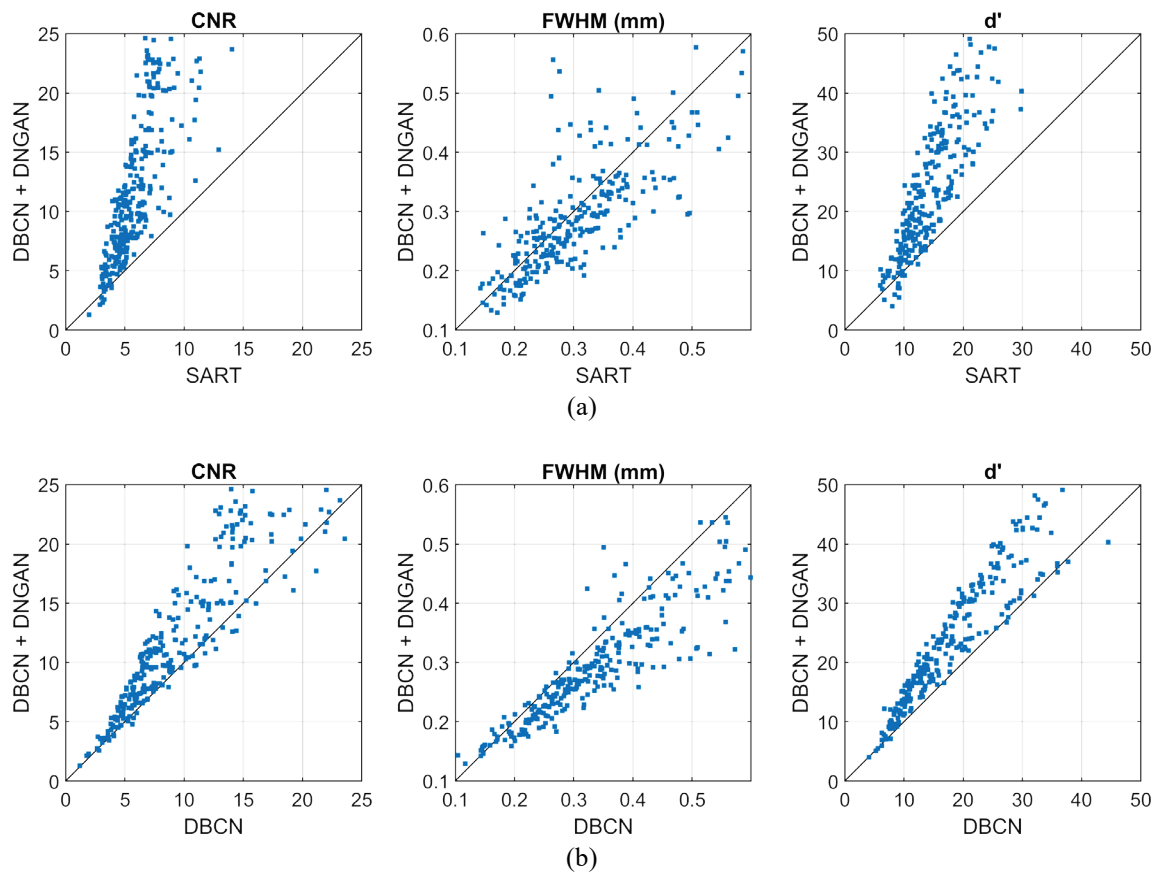


Figure 1. The scatter plots of CNR, FWHM, and  $d'$  for the MCs in the human subject data set. (a) DBCN+DNGAN vs. SART. (b) DBCN+DNGAN vs. DBCN.

Figure 2 illustrates the visual image quality of an MC cluster and a mass in two regions of interest. The example demonstrated the lower noise level of the background and the better conspicuity of MCs for DBCN+DNGAN than SART or DBCN, which was consistent with the quantitative results in Figure 1. The example of a spiculated mass

demonstrated that the tissue texture was smoother, and the mass margins remained satisfactory in the DBCN+DNGAN reconstructed images.

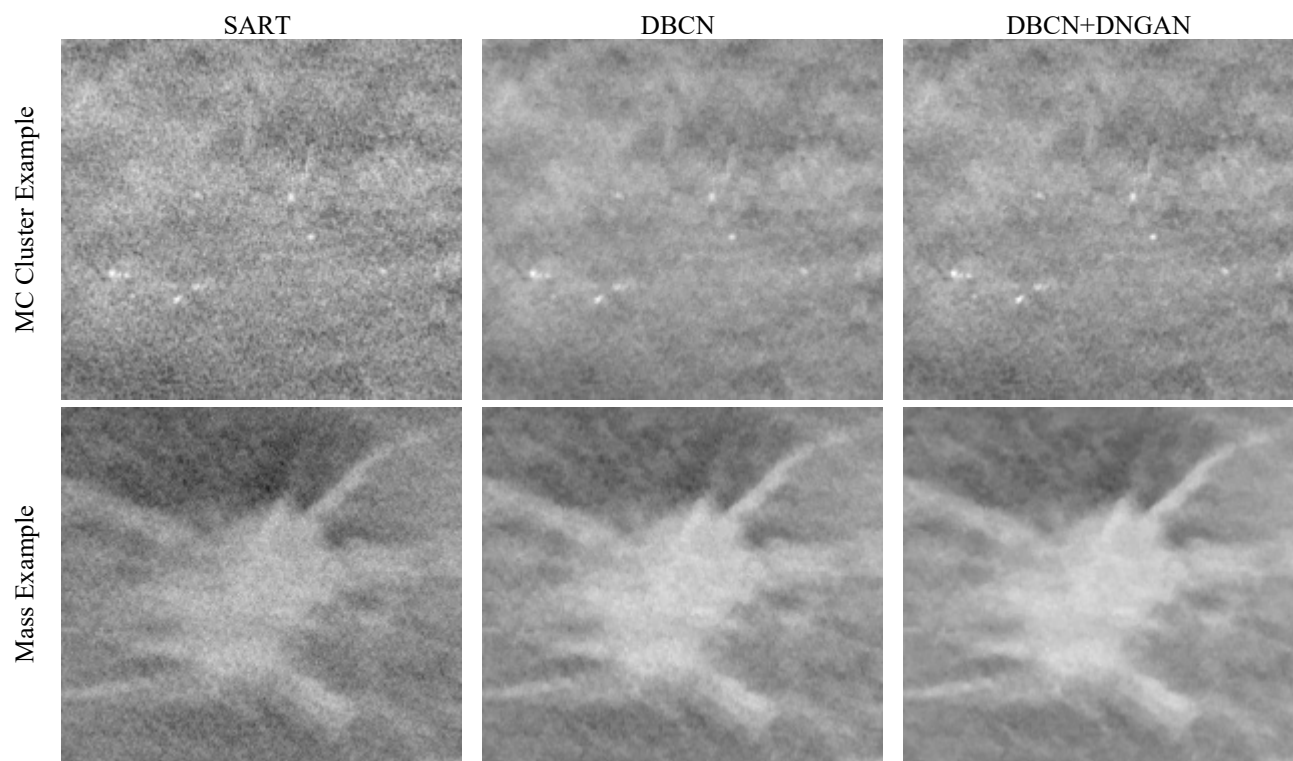


Figure 2. Example images of human subject DBTs with a ductal carcinoma in situ (MC cluster) and an invasive ductal carcinoma (spiculated mass). The focal planes of some of the MCs are not on this slice so they appeared blurred. The images show a  $20 \text{ mm} \times 18 \text{ mm}$  region. The images in the same row are displayed with the same window/level settings.

#### 4 DISCUSSION AND CONCLUSION

We proposed to combine DBCN and DNGAN for DBT reconstruction. DBCN is physics-based and considers the noise statistics of the image acquisition process to reconstruct DBT images. DNGAN is a data-driven DCNN method and was shown to be effective for denoising DBT images. We unified the two methods using the RED reconstruction framework and solved the optimization problem using the proximal gradient method. We demonstrated that the new DBCN+DNGAN method effectively improved the CNR and  $d'$  for the MCs in a small set of human subject DBTs in comparison to DBCN or SART in this feasibility study. The MCs were also sharper, as indicated by the lower FWHM values. The background noise level was reduced, and the soft tissue appearance was well preserved according to our visual judgement on the DBCN+DNGAN reconstructed images.

We observed that some noise specks or fibrous tissue edges were falsely enhanced in the DBCN+DNGAN-reconstructed images, which may cause false positive detection of MCs. Our next step is to deploy computerized detection programs and take into account any false enhancements in the evaluation and to optimize the reconstruction method and parameters. Future work also includes further improving the visibility of subtle MCs in the reconstructed DBTs and testing the reconstruction approach on a larger patient cohort.

#### ACKNOWLEDGMENT

This work is supported by the National Institutes of Health under Award Number R01 CA214981.

## REFERENCES

- [1] J. T. Dobbins, “Tomosynthesis imaging: at a translational crossroads,” *Medical Physics*, vol. 36, no. 6, pp. 1956–1967, May 2009, DOI: 10.1118/1.3120285.
- [2] M. Katsura, I. Matsuda, M. Akahane, J. Sato, H. Akai, K. Yasaka, A. Kunimatsu, and K. Ohtomo, “Model-based iterative reconstruction technique for radiation dose reduction in chest CT: comparison with the adaptive statistical iterative reconstruction technique,” *European Radiology*, vol. 22, no. 8, pp. 1613–1623, Aug. 2012, DOI: 10.1007/s00330-012-2452-z.
- [3] J. Zheng, J. A. Fessler, and H.-P. Chan, “Detector blur and correlated noise modeling for digital breast tomosynthesis reconstruction,” *IEEE Transactions on Medical Imaging*, vol. 37, no. 1, pp. 116–127, Jan. 2018, DOI: 10.1109/TMI.2017.2732824.
- [4] M. Gao, J. A. Fessler, and H.-P. Chan, “Deep convolutional neural network with adversarial training for denoising digital breast tomosynthesis images,” *IEEE Transactions on Medical Imaging*, vol. 40, no. 7, pp. 1805–1816, Jul. 2021, DOI: 10.1109/TMI.2021.3066896.
- [5] M. Gao, J. A. Fessler, and H.-P. Chan, “Digital breast tomosynthesis denoising using deep convolutional neural network: effects of dose level of training target images,” in *Proceedings of SPIE*, 2021, 115951K, DOI: 10.1117/12.2580900.
- [6] J. Zheng, J. A. Fessler, and H.-P. Chan, “Effects of detector blur and correlated noise on digital breast tomosynthesis reconstruction,” in *Proceedings of SPIE*, 2017, 1013226, DOI: 10.1117/12.2255689.
- [7] Y. Romano, M. Elad, and P. Milanfar, “The little engine that could: regularization by denoising (RED),” *SIAM Journal on Imaging Sciences*, vol. 10, no. 4, pp. 1804–1844, Jan. 2017, DOI: 10.1137/16M1102884.
- [8] E. T. Reehorst and P. Schniter, “Regularization by Denoising: Clarifications and New Interpretations,” *IEEE Transactions on Computational Imaging*, vol. 5, no. 1, pp. 52–67, Mar. 2019, DOI: 10.1109/TCI.2018.2880326.
- [9] A. Badano, C. G. Graff, A. Badal, D. Sharma, R. Zeng, F. W. Samuelson, S. J. Glick, and K. J. Myers, “Evaluation of digital breast tomosynthesis as replacement of full-field digital mammography using an in silico imaging trial,” *JAMA Network Open*, vol. 1, no. 7, p. e185474, Nov. 2018, DOI: 10.1001/jamanetworkopen.2018.5474.